AIAA JOURNAL
Vol. 42, No. 11, November 2004

Near-Critical Swirling Flow in a Slightly Contracting Pipe

Z. Rusak* and C. C. Meder†
Rensselaer Polytechnic Institute, Troy, New York 12180-3590

The development of an inviscid, incompressible, axisymmetric, and near-critical swirling jet entering a slightly contracting finite-length pipe is studied. Certain flow conditions that can reflect the physical situation are prescribed along the pipe inlet, outlet, centerline, and wall. To understand the nature of the flows near the critical swirl level, a nonlinear small-disturbance analysis is developed from the governing equations of motion. It shows that a small but finite pipe contraction causes the flow to accelerate near the centerline and decelerate along the wall. For certain inlet swirl levels and pipe contractions, the flow on the wall at the pipe outlet can stagnate. The analysis indicates for the first time that a wall separation zone can appear in pipes at rotation levels below the critical swirl for vortex breakdown and compete with the appearance of the breakdown zones. Increasing the vortex core radius, the speed of the axial jet, and the pipe length promotes the wall separation phenomenon at swirl levels below the critical swirl for a fixed pipe contraction or at a smaller pipe contraction for a fixed swirl level. Based on the present results and previous studies, the interaction between wall separation zones and vortex breakdown zones is discussed. This investigation might be relevant for high-Reynolds-number laminar flows in pipes and as long as the boundary layers remain thin and attached to the pipe wall.

I. Introduction

THE study of the dynamics of rotating flows in pipes has various technological applications for areas such as combustion, chemical mixing or separation processes, and the design of nozzles behind turbines. Of specific interest is the investigation of the appearance of instabilities and breakdown phenomena in such flows (for example, see the review papers by Hall,[1] Leibovich,[2] Escudier,[3] Sarpkaya,[4] and Rusak[5]). These are characterized by the appearance of disturbances in the flow when the swirl level is relatively high. The disturbances can range from weak helical waves to the strong spiral or nearly axisymmetric breakdown (separation) zones around the pipe centerline.

In some of the devices, the geometry of the pipe diverges, and in other cases it contracts. These changes in pipe geometry can affect the dynamics of the vortex flow. For example, pipe divergence helps to promote the vortex breakdown phenomena by inducing an adverse pressure gradient (see the experiments described in Refs. 2–4). On the other hand, pipe contraction is used to accelerate the flow and delay the appearance of breakdown to higher levels of swirl.

Vortex flows in diverging pipes were studied by Batchelor[6] and Buntine and Saffman,[7] who developed families of steady-state solutions at various levels of swirl and pipe divergence. Buntine and Saffman[7] showed through numerical computations that at certain swirl levels the flow near the centerline can decelerate to stagnation, resulting in separation (breakdown) zones. Rusak et al.[8] have recently developed asymptotic solutions that match with those of Batchelor[6] and Buntine and Saffman[7] and clarify the relationship between these works and the critical swirl level ω_c of Benjamin[9] and the solitary wave solutions of Leibovich and Kribus.[10] It was found that a small but finite pipe divergence breaks the transcritical bifurcation of solutions of a flow in a straight pipe into two equilibrium solution branches. These branches fold at limit swirl levels $\omega_{c\sigma 1} < \omega_c$ and $\omega_{c\sigma 2} > \omega_c$ around the critical swirl ω_c, resulting in a finite gap of swirl that separates the two branches. This suggests that no near-columnar axisymmetric state can exist within the range of incoming swirl between $\omega_{c\sigma 1}$ and $\omega_{c\sigma 2}$; the flow must develop large disturbances in this swirl range. When the pipe divergence is sufficiently small, there exists a certain range of swirl where two steady states can appear under the same inlet/outlet conditions, one which is a near-columnar state and the other is a solitary wave state. However, when the pipe divergence is increased this special behavior uniformly changes into a branch of solutions with no fold. The results also show that increasing the pipe divergence decreases the critical swirl for vortex breakdown and helps to decelerate the flow near the centerline at lower levels of swirl. Therefore, pipe divergence promotes breakdown.

In a recent work, Rusak and Judd[11] have studied the linear stability of the various solutions found in Rusak et al.[8] They showed that the limit levels of swirl $\omega_{c\sigma 1}$ and $\omega_{c\sigma 2}$ where fold occurs are points of exchange of stability. The near-columnar states are stable to a certain mode of disturbance, whereas the solitary wave states are unstable. These results shed light on the dynamics of vortex flows in a diverging pipe and the transition to vortex breakdown. Also note that Wang and Rusak[12] developed a theory for the vortex breakdown process in a straight pipe and showed that in a long pipe the critical swirl ω_c is a point of exchange of stability. Vortex flows with swirl level above ω_c are unstable, must develop a breakdown process, and evolve into axisymmetric breakdown states. The numerical simulations of Rusak et al.[13] demonstrate the breakdown process and the transition to axisymmetric breakdown states.

The study of rotating flows in contracting pipes is limited to the solutions of Batchelor,[6] which show the acceleration of the flow along the centerline. In the case of contracting pipes, these solutions do not indicate for any possible instability or separation phenomena in the flow. Yet, it is clear that as the swirl is increased, the flow acceleration near the centerline causes, from the balance of mass, a flow deceleration near the wall. Sufficiently high swirl levels of the entering vortex jet can result in stagnation on the wall and the establishment of a flow separation zone near the wall with reversed axial speeds inside the zone. Such flow states were never investigated before. Moreover, the appearance of separation zones on the pipe wall can compete with the appearance of the breakdown zones near the centerline. In certain situations, the wall separation zones can appear at swirl levels below the critical value for vortex breakdown and can dominate the flow behavior. Such a phenomenon was never studied before, neither experimentally nor numerically. Moreover, it probably occurred in some experiments of swirling flows without any attention to it. It is only the study of Mourtazin[14] that reports

Presented as Paper 2002-2984 at the 3rd Theoretical Fluid Mechanics Meeting, St. Louis, MO, 24–26 June 2002; received 24 January 2004; revision received 15 June 2004; accepted for publication 26 June 2004.

*Professor, Department of Mechanical, Aerospace, and Nuclear Engineering; rusakz@rpi.edu. Associate Fellow AIAA.

†Undergraduate Student, Department of Mechanical, Aerospace, and Nuclear Engineering; currently Aeronautical Engineer, Boeing Commercial Airplanes, The Boeing Company, Everett, WA 98204.

about the appearance of large-amplitude standing waves adjacent to the pipe wall at swirl levels below those where vortex breakdown was observed. As vortex breakdown suddenly appeared in the pipe with the increase of the incoming swirl level, these standing waves disappeared.

Therefore, the flow of vortex jets in contracting pipes is an important problem to investigate because it can be a typical situation in variety of technological flow apparatuses that use vortex flows or that investigate the vortex breakdown phenomenon. The present analysis extends the previous work of Rusak et al.[8] on swirling flows in a slightly diverging pipe to the case of a contracting pipe. A nonlinear small-disturbance analysis is developed for near-critical swirling flows (incoming vortex jets with swirl level around ω_c). The results show that pipe contraction helps to delay the appearance of vortex breakdown near the pipe centerline to higher swirl levels. It also indicates for the first time that pipe contraction can induce wall-separation zones above a certain swirl level denoted as ω_{ws}. At certain pipe contractions, ω_{ws} might even be less than ω_c, and then the wall zones might appear before the onset of the centerline vortex breakdown zones. It is also found that increasing the vortex core radius, the speed of the axial jet entering the pipe, and the pipe length promotes the wall separation phenomenon at swirl levels below the critical swirl for breakdown or at a smaller pipe contraction for a fixed swirl level.

The present study concentrates on inviscid swirling flows in a contracting pipe. Yet, it can correctly represent the global behavior of high-Reynolds-number laminar flows in finite-length pipes. The wall viscous boundary layers in such flows are very thin compared to the pipe radius, and as long as the boundary layers are attached to the wall the flow behavior in the pipe (outside the boundary layers) is dominated by the inviscid solution. Also, the boundary-layer's flow is strongly affected by the outer inviscid flow and can be analyzed by an asymptotic multiple-scale analysis, which is beyond the scope of the current study.

The present study predicts the development of a wall separation phenomenon as the incoming swirl level is increased toward ω_{ws}. This a result of the nonlinear interaction between the near-critical swirling flow dynamics and the pipe contraction. Such a dynamical behavior dominates the flow structure much beyond the boundary-layer's region. Therefore, the conditions for the first appearance of wall separation zones in the flow can be correctly predicted by the present inviscid flow analysis. These are specifically important when the wall zones appear at swirl levels below those at which vortex breakdown states evolve. However, the present inviscid small-disturbance analysis is limited to swirl levels below ω_{ws} and only indicates the appearance of the wall zones. It is not relevant for swirl levels above ω_{ws}, where the perturbation is large and the flow inside the wall separation zone and around it is strongly dominated by viscous effects.

II. Mathematical Model

A steady and axisymmetric flow with swirl is considered in a finite-length pipe with a small contraction. The flow is assumed inviscid and incompressible. These assumption can be relevant for high-Reynolds-number laminar flows and as long as the boundary layers remain thin and attached to the pipe wall. The pipe centerline is the x axis, where $0 \le x \le x_0$. The axial and radial distances are rescaled with the radius of the pipe inlet. The pipe wall is described by $R(x) = 1 - \lambda R_0(x)$, where λ is a measure of the pipe contraction and in our case $0 \le \lambda \ll 1$. The function $R_0(x)$ represents the pipe shape, and we assume $R_0(0) = 0$ and $R_0(x) > 0$ for $0 < x \le x_0$. In addition, at the pipe outlet we assume that the pipe shape slope vanishes, $R_{0x}(x_0) = 0$.

The axisymmetry of the problem allows the use of a stream function $\psi(x, y)$, where $y = r^2/2$, the radial velocity is $u = -\psi_x/\sqrt{(2y)}$, and the axial velocity is $w = \psi_y$. The azimuthal vorticity is $\eta = \sqrt{(2y)}\chi$, where $\chi = -(\psi_{yy} + \psi_{xx}/2y)$. The circulation function is $K = rv$, where v is the circumferential velocity. The stream function ψ, the circulation K, and the function χ are related through the following equations[12]:

$$\{\psi, K\} = 0, \qquad \{\psi, \chi\} = (1/4y^2)(K^2)_x \tag{1}$$

Here the Poisson brackets $\{\psi, K\}$ and $\{\psi, \chi\}$ are defined by

$$\{\psi, K\} = \psi_y K_x - \psi_x K_y, \qquad \{\psi, \chi\} = \psi_y \chi_x - \psi_x \chi_y \tag{2}$$

We study the flow in a pipe with a specific set of conditions posed on the boundaries. To satisfy the axisymmetric condition, we choose $\psi(x, 0) = 0$ along the pipe centerline. From conservation of mass, the pipe wall is a streamline where $\psi[x, R^2(x)/2] = \Psi_0$ for $0 \le x \le x_0$. Here Ψ_0 is the volume flux entering the pipe. Also, let

$$\psi(0, y) = \psi_0(y), \qquad K(0, y) = K_0(y) = \omega \tilde{K}_0(y) \quad \text{for} \quad 0 \le y \le \tfrac{1}{2} \tag{3}$$

be given along the inlet. In Eq. (3), ψ_0 is related to the inlet axial velocity profile, $w(0, y) = \psi_{0y}$, ω represents the swirl ratio of the incoming vortex flow, and $\tilde{K}_0$ is related to the inlet circumferential velocity profile $v(0, y) = \omega \tilde{K}_0/\sqrt{(2y)}$. From the conservation of mass, $\psi_0(\frac{1}{2}) = \Psi_0$. The inlet azimuthal vorticity is given by

$$\chi(0, y) = \chi_0(y) = -\psi_{0yy} \qquad \text{for} \qquad 0 \le y \le \tfrac{1}{2} \tag{4}$$

These inlet conditions can describe the incoming swirling flow to a pipe that is supplied by a vortex generator ahead of the pipe at a steady operation.

We also assume no radial velocity along the pipe outlet $x = x_0$, that is,

$$\psi_x(x_0, y) = 0 \qquad \text{for} \qquad 0 \le y \le y_0 \tag{5}$$

where $y_0 = [1 - \lambda R_0(x_0)]^2/2$. This outlet condition reflects an expected columnar state that can occur in long pipes where $x_0 \gg 1$.

Boundary conditions (3–5) were used in Wang and Rusak[12] and Rusak et al.[13] in their study of swirling flows in a straight pipe, in Rusak et al.[8] in their study of vortex flows in a diverging pipe, and in numerical simulations of the axisymmetric vortex breakdown.[15–17]

III. Small-Disturbance Approach

We expect that the flow disturbances created by the small pipe contraction ($0 \le \lambda \ll 1$) are relatively small compared to the base flow properties. Yet, the previous study by Rusak et al.[8] on flows in diverging pipes showed that when the swirl level ω of the incoming vortex flow is around the critical level ω_c the flow perturbations also depend on the swirl difference from the critical level $\Delta\Omega = \Omega - \Omega_c$. (Here we define $\Omega = \omega^2$.) It was also found that in the leading order the flow perturbations are much greater than the measure of the pipe divergence as well as $\Delta\Omega$. A similar situation is expected in the case of a contracting pipe. Therefore, when $0 \le \lambda \ll 1$ and $|\Delta\Omega|/\Omega_c \ll 1$ we consider a small perturbation solution of Eqs. (1–5) of the form

$$\begin{aligned}
\psi(x, y) &= \psi_0(y) + \epsilon_1(\lambda, \Delta\Omega)\psi_1(x, y) \\
&\quad + \epsilon_2(\lambda, \Delta\Omega)\psi_2(x, y) + \cdots \\
K(x, y) &= K_0(y) + \epsilon_1(\lambda, \Delta\Omega)K_1(x, y) \\
&\quad + \epsilon_2(\lambda, \Delta\Omega)K_2(x, y) + \cdots \\
\chi(x, y) &= \chi_0(y) + \epsilon_1(\lambda, \Delta\Omega)\chi_1(x, y) \\
&\quad + \epsilon_2(\lambda, \Delta\Omega)\chi_2(x, y) + \cdots \\
\chi_1 &= -(\psi_{1yy} + \psi_{1xx}/2y), \qquad \chi_2 = -(\psi_{2yy} + \psi_{2xx}/2y)
\end{aligned} \tag{6}$$

where we assume that $|\epsilon_1(\lambda, \Delta\Omega)| \ll 1$, $|\epsilon_2| \ll |\epsilon_1|$, but $0 \le \lambda \ll |\epsilon_1|$, $|\Delta\Omega| \ll |\epsilon_1|$, and $|\epsilon_1\lambda| \ll |\epsilon_2|$. In Eqs. (6), ψ_1 and ψ_2 represent the first-and second-order perturbations of the stream function; K_1 and K_2 represent the related perturbations of the circulation function; and χ_1 and χ_2 represent the related azimuthal vorticity perturbations.

The boundary conditions (3–5) show that the perturbations should satisfy the following conditions:

$$\psi_1(0,y)=0, \qquad K_1(0,y)=0, \qquad \psi_{1xx}(0,y)=0 \quad \text{for} \quad 0\le y\le y_0$$
$$\psi_{1x}(x_0,y)=0 \quad \text{for} \quad 0\le y\le \tfrac{1}{2}$$
$$\psi_1(x,0)=0 \quad \text{for} \quad 0\le x\le x_0 \tag{7}$$

$$\psi_2(0,y)=0, \qquad K_2(0,y)=0, \qquad \psi_{2xx}(0,y)=0 \quad \text{for} \quad 0\le y\le \tfrac{1}{2}$$
$$\psi_{2x}(x_0,y)=0 \quad \text{for} \quad 0\le y\le \tfrac{1}{2}$$
$$\psi_2(x,0)=0 \quad \text{for} \quad 0\le x\le x_0 \tag{8}$$

Also, the flow tangency condition along the pipe wall {which is given by $y=y_0(x)=R^2(x)/2=[1-\lambda R_0(x)]^2/2$} can be written as $u[x,\, y=y_0(x)]=R'(x)w[x,\, y=y_0(x)]$ or as

$$-\frac{\psi_x[x,\, y=y_0(x)]}{R(x)}=R'(x)\psi_y[x,\, y=y_0(x)]$$

where $R'(x)=\mathrm{d}R/\mathrm{d}x$. Expanding the various terms in this condition in a Taylor series and using the asymptotic expansions (6) gives

$$-\epsilon_1\psi_{1x}\left(x,\tfrac{1}{2}\right)-\epsilon_1\lambda\psi_{1xy}\left(x,\tfrac{1}{2}\right)R_0(x)-\epsilon_2\psi_{2x}\left(x,\tfrac{1}{2}\right)+\cdots$$
$$=-\lambda R_0'(x)\psi_{0y}\left(\tfrac{1}{2}\right)+\cdots$$

for $0\le x\le x_0$. The assumption $0<\lambda\ll|\epsilon_1|$ results in the following wall conditions:

$$\psi_{1x}\left(x,\tfrac{1}{2}\right)=0, \qquad \epsilon_2\psi_{2x}\left(x,\tfrac{1}{2}\right)=\lambda R_0'(x)\psi_{0y}\left(\tfrac{1}{2}\right)$$

for $0\le x\le x_0$ or when we integrate these conditions with x we have

$$\psi_1\left(x,\tfrac{1}{2}\right)=0, \qquad \epsilon_2\psi_2\left(x,\tfrac{1}{2}\right)=\lambda R_0(x)\psi_{0y}\left(\tfrac{1}{2}\right) \quad \text{for} \quad 0\le x\le x_0 \tag{9}$$

Following Rusak et al.,[8] the substitution of expansions (6) into Eqs. (1) and (2) gives from the leading order $\mathcal{O}(\epsilon_1)$ equations:

$$\psi_{1yy}+\frac{\psi_{1xx}}{2y}+\left(\frac{\chi_{0y}}{\psi_{0y}}+\frac{\Omega_c\tilde{K}_0\tilde{K}_{0y}}{2y^2\psi_{0y}^2}\right)\psi_1=0 \tag{10}$$

with the following boundary conditions:

$$\psi_1(x,0)=0, \qquad \psi_1\left(x,\tfrac{1}{2}\right)=0 \quad \text{for} \quad 0\le x\le x_0 \tag{11}$$

$$\psi_1(0,y)=0, \qquad \psi_{1xx}(0,y)=0 \quad \text{for} \quad 0\le y\le \tfrac{1}{2} \tag{12}$$

The solution of Eqs. (10–12) with the relevant (longest) wave length is

$$\psi_1=\psi_{1c}(x,y)=\Phi(y)\sin[(\pi/2x_0)x] \tag{13}$$

where $\omega_c=\sqrt{(\Omega_c)}$ is the critical swirl and Φ is the eigenfunction that corresponds to the critical state. Both depend on x_0 and the properties of $\psi_0(y)$ and $\tilde{K}_0(y)$ and are found from the solution of the following eigenvalue problem:

$$\Phi_{yy}+\left(-\frac{\pi^2}{8x_0^2y}+\frac{\chi_{0y}}{\psi_{0y}}+\frac{\Omega_c\tilde{K}_0\tilde{K}_{0y}}{2y^2\psi_{0y}^2}\right)\Phi=0$$
$$\Phi(0)=0, \qquad \Phi\left(\frac{1}{2}\right)=0 \tag{14}$$

From the theory of partial differential equations, it can be shown that the problem (14) has a nontrivial solution only for the certain swirl levels that are the eigenvalues $\Omega_1, \Omega_2, \ldots$ of the problem. We defined in Wang and Rusak[12] the first eigenvalue Ω_1 as the "critical level of swirl for a finite length pipe," that is, $\omega_c^2=\Omega_c=\Omega_1$. The critical swirl ω_c is actually the transcritical bifurcation point of the steady-state equations of motion, which has been discussed in Wang and Rusak's[12] theory of vortex breakdown. Notice from Eqs. (14) that as x_0 tends to infinity ω_c tends to the critical swirl ω_{cB}, as was defined by Benjamin.[9]

The solution (13) provides the shape of the stream function perturbation ψ_1 from which the shape of the circulation perturbation $K_1=K_{1c}=(\omega_c\tilde{K}_{0y}/\psi_{0y})\psi_{1c}$ and the azimuthal vorticity perturbation χ_1 can be computed. Yet, the size of these perturbations ϵ_1, which can be related to the swirl difference $\Delta\Omega$ and the pipe contraction λ, has to be computed. To find $\epsilon_1(\Delta\Omega,\lambda)$, we look at the second-order terms of Eqs. (1) and (2). Again, following Rusak et al.,[8] we find that

$$\epsilon_2\left[\psi_{0y}\chi_{2x}-\psi_{2x}\left(\chi_{0y}+\frac{\Omega_c\tilde{K}_0\tilde{K}_{0y}}{\psi_{0y}2y^2}\right)\right]$$
$$+\epsilon_1^2\left[-\frac{K_0(\psi_{1c}^2)_x}{4y^2}(K_{0yy}\psi_{0y}-K_{0y}\psi_{0yy})\frac{1}{\psi_{0y}^3}+\psi_{1cy}\chi_{1cx}\right.$$
$$\left.-\psi_{1cx}\chi_{1cy}-\frac{(K_{1c}^2)_x}{4y^2}\right]-\epsilon_1\Delta\Omega\left(\frac{\tilde{K}_0\tilde{K}_{0y}}{2y^2\psi_{0y}}\right)\psi_{1cx}=0$$

Using the following relationship from Eq. (10):

$$\chi_{1c}=\left(\frac{\chi_{0y}}{\psi_{0y}}+\frac{\tilde{K}_0\tilde{K}_{0y}}{\psi_{0y}^2 2y^2}\right)\psi_{1c}$$

rearranging terms, integrating with respect to x, and using the conditions (7) and (8) gives

$$\epsilon_2\left[\chi_2-\psi_2\left(\frac{\chi_{0y}}{\psi_{0y}}+\frac{\Omega_c\tilde{K}_0\tilde{K}_{0y}}{2y^2\psi_{0y}^2}\right)\right]$$
$$+\epsilon_1^2\left[-\frac{1}{2\psi_{0y}}\left(\frac{\chi_{0y}}{\psi_{0y}}+\frac{\Omega_c\tilde{K}_0\tilde{K}_{0y}}{2y^2\psi_{0y}^2}\right)_y\right.$$
$$\left.-\frac{\Omega_c\tilde{K}_0}{4y^2\psi_{0y}^4}(\tilde{K}_{0yy}\psi_{0y}-\tilde{K}_{0y}\psi_{0yy})-\frac{\Omega_c(\tilde{K}_{0y})^2}{4y^2\psi_{0y}^2}\right]\psi_{1c}^2$$
$$-\epsilon_1\Delta\Omega\left(\frac{\tilde{K}_0\tilde{K}_{0y}}{2y^2\psi_{0y}^2}\right)\psi_{1c}=0 \tag{15}$$

with corresponding boundary conditions (8) and (9).

Now, multiplying Eq. (15) by ψ_{1c}, integrating over the domain $(0\le x\le x_0,\, 0\le y\le\frac{1}{2})$, using Eqs. (8) and (9) for ψ_2 in the integration by parts, and applying Eq. (10) yields the following quadratic equation for solving ϵ_1:

$$\epsilon_1^2M_1-\epsilon_1\Delta\Omega M_2-\lambda M_3=0 \tag{16}$$

Here

$$M_1=-\int_0^{x_0}\int_0^{\frac{1}{2}}\left[\frac{1}{\psi_{0y}}\left(\frac{\chi_{0y}}{\psi_{0y}}\right)_y+\Omega_c\frac{1}{y\psi_{0y}^{\frac{3}{2}}}\left(\frac{\tilde{K}_0\tilde{K}_{0y}}{y\psi_{0y}^{\frac{3}{2}}}\right)_y\right]$$
$$\times\frac{\psi_{1c}^3}{2}\,\mathrm{d}y\,\mathrm{d}x=\frac{4x_0}{3\pi}N_1$$

$$M_2 = \int_0^{x_0}\int_0^{\frac{1}{2}} \frac{\tilde{K}_0\tilde{K}_{0y}}{2y^2\psi_{0y}^2}\psi_{1c}^2\,\mathrm{d}y\,\mathrm{d}x = \frac{1}{2}x_0N_2$$

$$M_3 = \left[-\Phi_y\left(\frac{1}{2}\right)\right]\psi_{0y}\left(\frac{1}{2}\right)\int_0^{x_0} R_0(x)\sin\left(\frac{\pi x}{2x_0}\right)\mathrm{d}x$$

$$= \frac{2x_0}{\pi}N_3 \tag{17}$$

where

$$N_1 = -\int_0^{\frac{1}{2}}\left[\frac{1}{\psi_{0y}}\left(\frac{\chi_{0y}}{\psi_{0y}}\right)_y + \Omega_c\frac{1}{y\psi_{0y}^{\frac{3}{2}}}\left(\frac{\tilde{K}_0\tilde{K}_{0y}}{y\psi_{0y}^{\frac{3}{2}}}\right)_y\right]\frac{\Phi^3(y)}{2}\,\mathrm{d}y$$

$$N_2 = \int_0^{\frac{1}{2}}\frac{\tilde{K}_0\tilde{K}_{0y}}{2y^2\psi_{0y}^2}\Phi^2(y)\,\mathrm{d}y$$

$$N_3 = \frac{\pi}{2x_0}\left[-\Phi_y\left(\frac{1}{2}\right)\right]\psi_{0y}\left(\frac{1}{2}\right)\int_0^{x_0} R_0(x)\sin\left(\frac{\pi x}{2x_0}\right)\mathrm{d}x \tag{18}$$

For relevant rotating base flows such as the Rankine vortex, the Burgers vortex, or the Q-vortex, it can be shown that N_1 and N_2 are positive. Also, because from its definition $R_0(x) > 0$ for all x and $\Phi_y(\frac{1}{2})$ is always negative then $N_3 > 0$. Therefore, with $\lambda > 0$, Eq. (16) has, for $\Delta\Omega$, two real solutions of ϵ_1

$$\epsilon_1(\lambda, \Delta\Omega) = \frac{\Delta\Omega M_2 \pm \sqrt{(\Delta\Omega)^2M_2^2 + 4\lambda M_1M_3}}{2M_1}$$

$$= \frac{\Delta\Omega N_2 \pm \sqrt{(\Delta\Omega)^2N_2^2 + 32\lambda N_1N_3/3\pi^2}}{8N_1/3\pi} \tag{19}$$

From Eqs. (6) we can obtain the asymptotic form of the stream function $\psi(x, y)$ for incoming flows with swirl near the critical swirl Ω_c:

$$\psi(x, y) = \psi_0(y) + \frac{\Delta\Omega N_2 \pm \sqrt{(\Delta\Omega)^2N_2^2 + 32\lambda N_1N_3/3\pi^2}}{8N_1/3\pi}$$

$$\times\,\Phi(y)\sin\left(\frac{\pi x}{2x_0}\right) + \mathcal{O}(\lambda) \tag{20}$$

Two primary parameters can characterize the flow states described by Eq. (20). These are the axial speed at the centerline of the pipe outlet ($x = x_0$):

$$w(x_0, 0) = \psi_{0y}(0) + \frac{\Delta\Omega N_2 \pm \sqrt{(\Delta\Omega)^2N_2^2 + 32\lambda N_1N_3/3\pi^2}}{8N_1/3\pi}$$

$$\times\,\Phi_y(0) + \mathcal{O}(\lambda) \tag{21}$$

and the axial speed on the wall at the pipe outlet ($x = x_0$):

$$w\left(x_0, \frac{1}{2}\right) = \psi_{0y}\left(\frac{1}{2}\right) + \frac{\Delta\Omega N_2 \pm \sqrt{(\Delta\Omega)^2N_2^2 + 32\lambda N_1N_3/3\pi^2}}{8N_1/3\pi}$$

$$\times\,\Phi_y\left(\frac{1}{2}\right) + \mathcal{O}(\lambda) \tag{22}$$

When $w(x_0, 0) \le 0$, a separation (breakdown) zone appears along the pipe centerline. However, in the present case it can be shown from Eq. (21) that $w(x_0, 0) > \psi_{0y}(0) > 0$ for the swirl range $0 \le \omega < \omega_c$, and, therefore, no breakdown zone can appear in this swirl range as a result of the pipe contraction. On the other hand, when $w(x_0, \frac{1}{2}) \le 0$ a separation zone appears along the pipe wall as a result of the pipe contraction. Because $\Phi_y(\frac{1}{2}) < 0$, we find from Eq. (22) that $w(x_0, \frac{1}{2})$ can become zero at a certain swirl ratio denoted by ω_{ws}. Although the present analysis is not relevant for swirl levels above ω_{ws}, it indicates that a wall separation zone appears when $\omega > \omega_{ws}$. Also, for pipe contractions λ above a certain value it is found that $\omega_{ws} < \omega_c$. Then it is expected that the pipe contraction might induce wall separation zones at incoming swirl levels that are lower than the sufficient critical swirl for vortex breakdown.

IV. Examples

The character of the flow states according to Eq. (20) is demonstrated for the case where the base flow is described by a Q-vortex model:

$$\psi_{0y}(y) = 1 + de^{-2by}, \qquad K_0(y) = \omega(1 - e^{-2by}),$$

$$\chi_0(y) = 2bde^{-2by} \tag{23}$$

Here the constant b is related to the vortex core radius as $r_c = 1.12/\sqrt{b}$, and the constant d is a measure of the axial jet/wake character of the inlet flow. The Q-vortex model characterizes experimental vortex flows at the inlet of a pipe (for example, see Leibovich[2]). The pipe shape function is given by $R_0(x) = 1 - \cos(\pi x/x_0)$.

Using a standard ordinary-differential-equation solver from MATLAB® for Eqs. (14), the eigenfunction $\Phi(y)$ is computed [where $\Phi_y(0) = 1$ is assumed]. Then an integration scheme is used to calculate the constants N_1 and N_2 according to Eqs. (18). For example, in the case of a Burgers vortex where $b = 1.0$, $d = 1.0$, $x_0 = 1.0$, it is found that $\omega_c = 4.6025$, $\Phi(\frac{1}{2}) = -0.3054$, $N_1 = 0.004175$, $N_2 = 0.003544$, and $N_3 = 0.5545$. Using Eqs. (21) and (22), we describe the bifurcation diagrams in terms of the parameters $w(x_0, 0)$ and $w(x_0, \frac{1}{2})$ (computed at the same states) as the swirl level ω is increased at various fixed values of the contraction parameter λ (see Figs. 1 and 2).

Figure 1 shows the change of $w(x_0, 0)$ with ω when $\lambda = 0$, 0.1. The transcritical bifurcation of solutions at $\omega_c = 4.6025$ when the pipe is straight ($\lambda = 0$) is evident from this figure (see also Wang and Rusak[12]). When $\lambda = 0.1$, it can be seen that the transcritical bifurcation of solutions changes into two branches of solutions. The first, for swirl levels below ω_c, is characterized by states where the pipe contraction induces a flow acceleration along the centerline and where the outlet speed $w(x_0, 0)$ increases with ω. The second branch is for swirl levels above ω_c and is characterized by flow states where the pipe contraction interacts with the high level of swirl in a nonlinear manner and a flow deceleration occurs along the pipe centerline. From the stability studies of Rusak and Judd,[11] it can be inferred that, when a similar study is conducted for the contracting pipe case, the states along the first branch are linearly stable, whereas those along the second branch are unstable.

Figure 2 describes the change of $w(x_0, \frac{1}{2})$ with ω when $\lambda = 0$, 0.1 for the same states computed in Fig. 1. For the stable states along the first branch in Fig. 1, the flow decelerates along the contracting pipe wall. As ω is increased with a fixed value of λ, the axial speed on the wall at the outlet decreases. At a certain swirl level, denoted as ω_{ws}, a stagnation point appears on the wall at the pipe outlet. For example, in the case when $b = d = 1$, $x_0 = 1$, and $\lambda = 0.1$ we find that $\omega_{ws} = 4.6025$, which is in this case very close to ω_c. It can also be seen from Fig. 2 that ω_{ws} decreases with the increase in the pipe contraction λ. For example, when $\lambda = 0.2$ we find that $\omega_{ws} = 4.33$, which is less than ω_c. It is expected that a wall separation zone can develop near the pipe outlet when $\omega > \omega_{ws}$. Figure 2 demonstrates that a wall separation phenomenon can occur under certain flow conditions and pipe contraction at swirl levels below the critical swirl for breakdown.

To illustrate the nature of the various stable solutions along the first branch, streamline contours are presented in Figs. 3a and 3b. In each figure the lower streamline represents the pipe centerline $\psi = 0$, the upper streamline represents the pipe wall $\psi = 1.131$, the flow runs from left to right, and there are 15 equispaced level curves of $\psi =$ constant with $\Delta\psi = 0.0754$. These contours are for the case where $b = d = 1$, $x_0 = 1$, and $\lambda = 0.1$.

Figure 3a, which corresponds to point (a) in Fig. 2, describes the flow state at $\omega = 2.3$. This is a nearly columnar state where the swirling flow is constricted by the pipe wall, slightly accelerated along the centerline, and slightly decelerated along the pipe

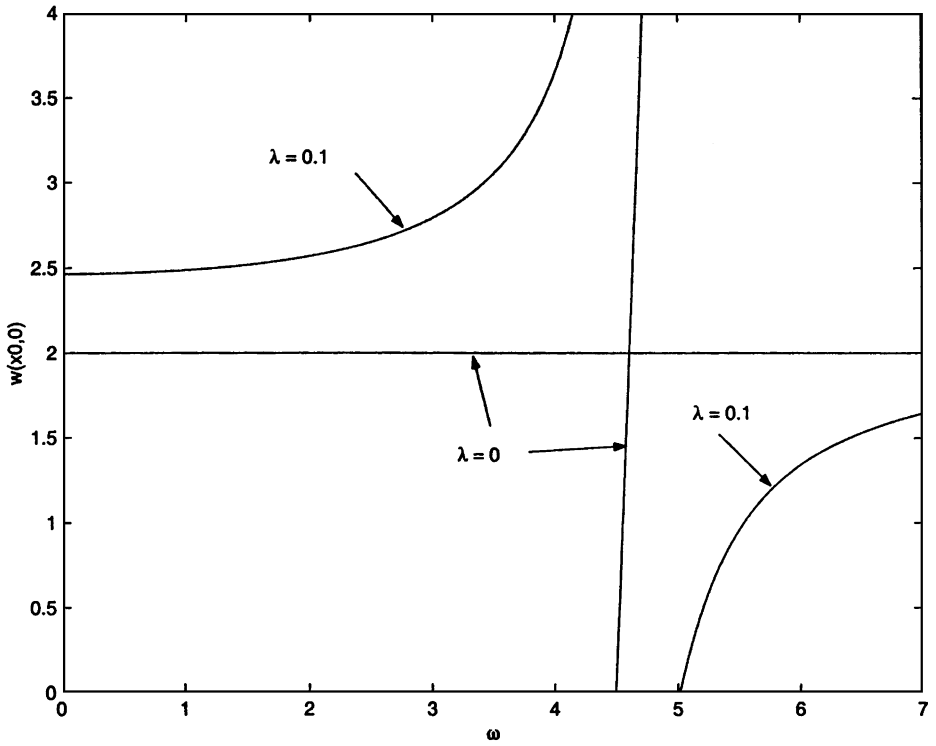

Fig. 1 Axial speed at the outlet centerline as a function of the swirl level for a Q vortex [Eq. (23)] with $b = d = 1.0$ in a straight pipe ($\lambda = 0.0$) and in a contracting pipe with $\lambda = 0.1$ and $x_0 = 1.0$.

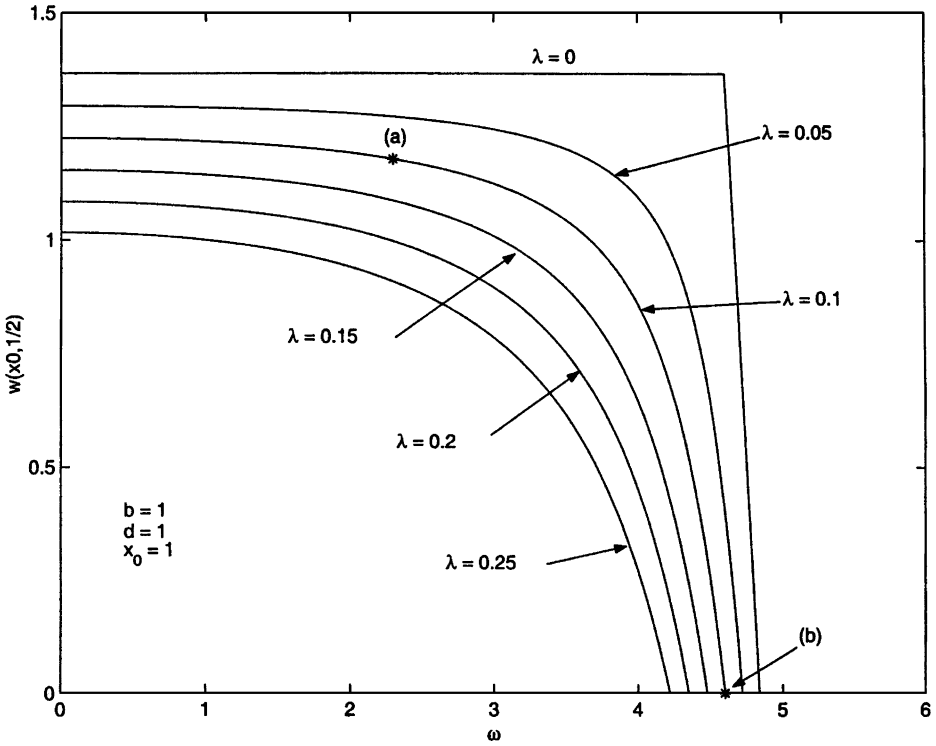

Fig. 2 Axial speed at the outlet wall as a function of the swirl level for a Q vortex [Eq. (23)] with $b = d = 1.0$ in a straight pipe ($\lambda = 0.0$) and in various contracting pipes with $x_0 = 1.0$.

wall. Figure 3b, which corresponds to point (b) in Fig. 2, describes the flow state at $\omega = 4.6025$. This is a state where the nonlinear interaction between the near-critical swirl and the pipe contraction results in a significant flow acceleration along the centerline and a stagnation point on the pipe wall at the outlet. This indicates that $\omega_{ws} \sim 4.603$. Also, notice the divergence of streamlines from the wall near the pipe outlet in this state. Figure 3c describes the flow state at $\omega = 4.8 > \omega_{ws}$, where it is predicted that a separation zone appears along the pipe wall. It should be clarified here that the present inviscid small-disturbance analysis is not relevant for swirl levels above ω_{ws}, where the perturbation is not small any more and the flow inside the induced separation zones and around them is strongly dominated by viscous effects.

The results of Fig. 2 provide the values of ω_{ws} as function of λ (see Fig. 4). It can be seen that as λ decreases ω_{ws} increases. Also

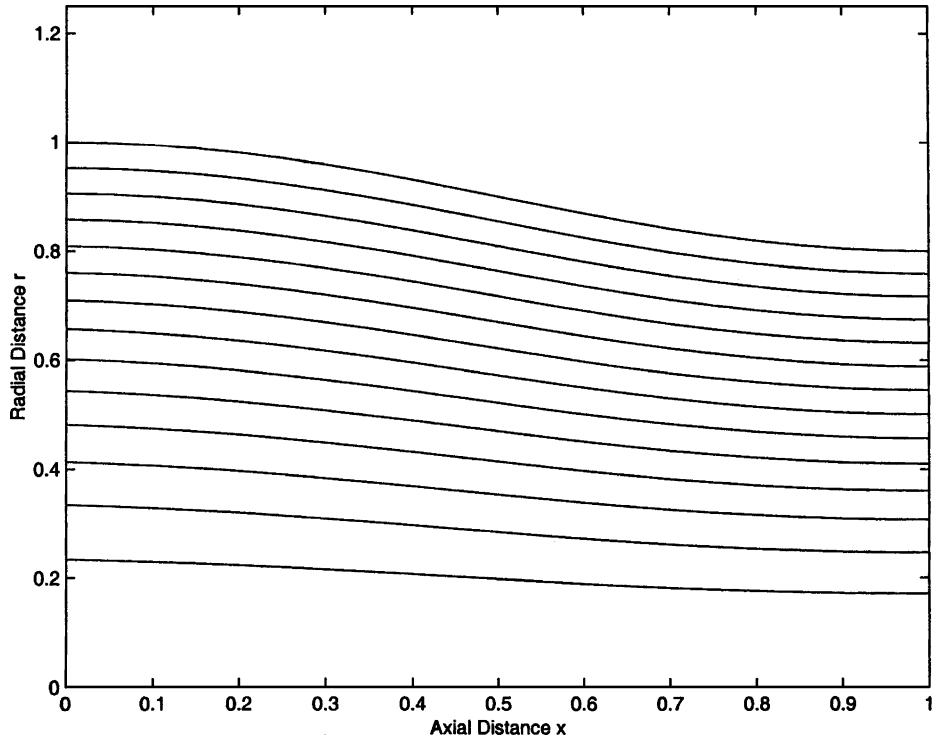

Fig. 3a Streamline contours of the flow state for an incoming Q vortex [Eq. (23)] with $b = d = 1.0$ and $\omega = 2.3$ in a contracting pipe with $\lambda = 0.1$ and $x_0 = 1.0$.

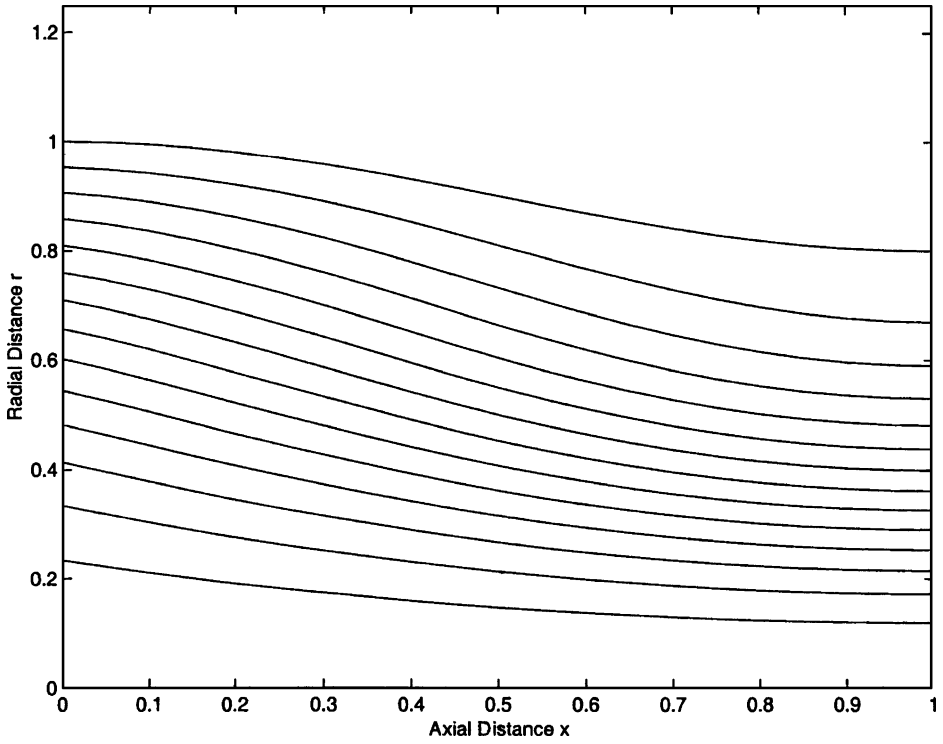

Fig. 3b Streamline contours of the flow state for an incoming Q vortex [Eq. (23)] with $b = d = 1.0$ and $\omega = 4.6025$ in a contracting pipe with $\lambda = 0.1$ and $x_0 = 1.0$.

shown in this figure is the critical level for breakdown of the given inlet vortex flow $\omega_c = 4.6025$. The figure demonstrates that there is a range of the pipe contraction λ where wall separation zones can appear at swirl levels below those sufficient for the appearance of breakdown.

Figure 5 describes the values of ω_{ws} as function of λ for an incoming vortex flow with $b = 1$, $d = 2$, and $x_0 = 1$. It can be seen that the increase in the inlet jet speed can result in wall separation at lower values of the pipe contraction. The parametric maps in Figs. 4 and 5 can be used to identify the conditions for the appearance of vortex breakdown or wall separation in the pipe.

We denote λ_c as the value of λ that is needed to find a wall separation at the critical swirl ω_c. Note that ω_c is a function of d and b, and it increases with the increase in d and decrease in b. Figure 6 describes the values of λ_c as a function of the jet parameter d for a fixed core radius ($b = 1$) and fixed values of the

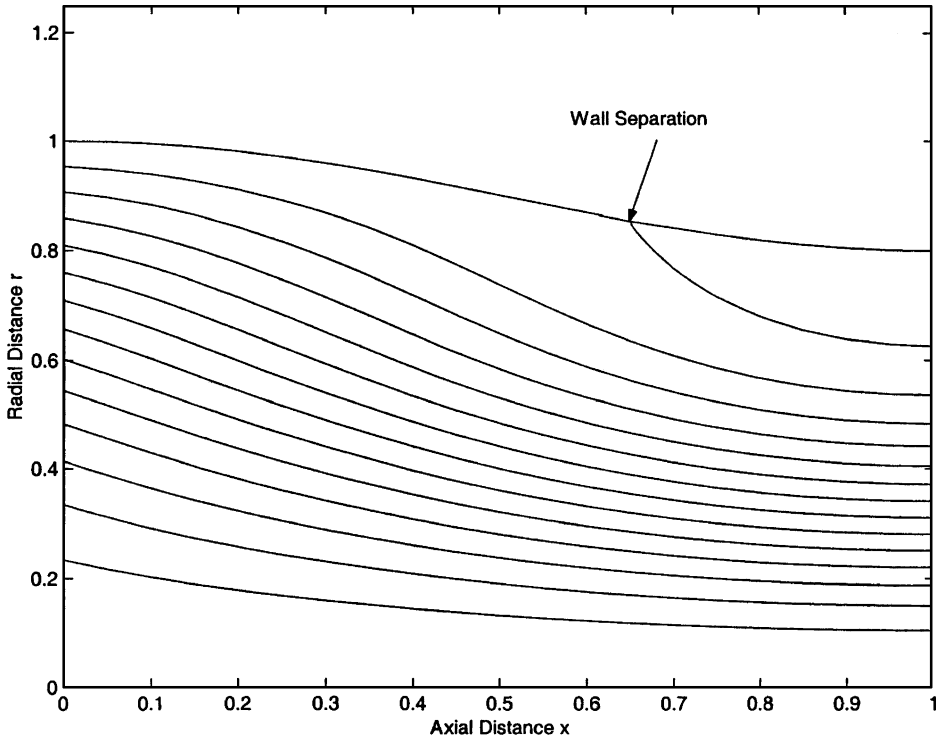

Fig. 3c Streamline contours of the flow state for an incoming Q vortex [Eq. (23)] with $b = d = 1.0$ and $\omega = 4.8$ in a contracting pipe with $\lambda = 0.1$ and $x_0 = 1.0$.

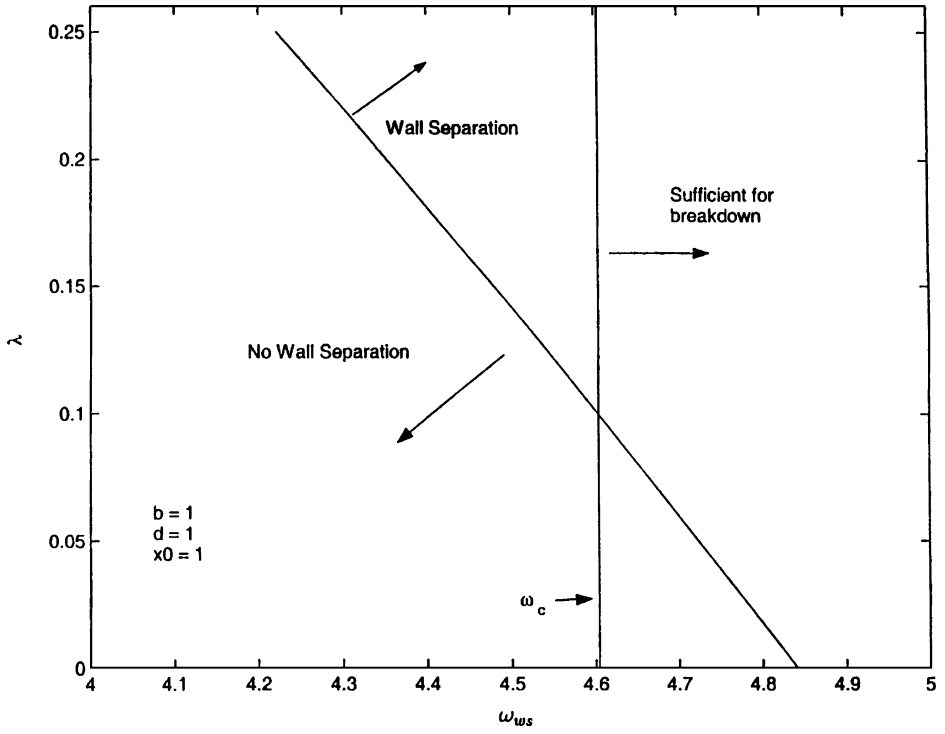

Fig. 4 Pipe contraction λ against the swirl level for wall separation ω_{ws} for an incoming Q vortex [Eq. (23)] with $b = d = 1.0$ in a pipe with $x_0 = 1.0$.

pipe length, $x_0 = 1$, 10. Note that when $\lambda > \lambda_c$ wall separation appears at swirl levels below ω_c. It can be seen that λ_c decreases with increasing d. This means that less pipe contraction is needed to find wall separation in vortex flows when the axial jet speed is higher. It is also found that increasing the pipe length reduces λ_c at a fixed value of d. This means that less pipe contraction is needed to find wall separation in vortex flows when the pipe length is greater.

Figure 7 describes the values of λ_c as a function of the vortex core radius r_c for a fixed jet parameter ($d = 2$) and fixed values of the pipe length, $x_0 = 1$, 10. Note that again when $\lambda > \lambda_c$ wall separation appears at swirl levels below ω_c. Also note that ω_c increases with the increase in r_c. It can be seen that λ_c decreases with increasing r_c. This means that less pipe contraction is needed to find wall separation in vortex flows when the core size is larger. As in Fig. 6, it is found that increasing the pipe length reduces λ_c

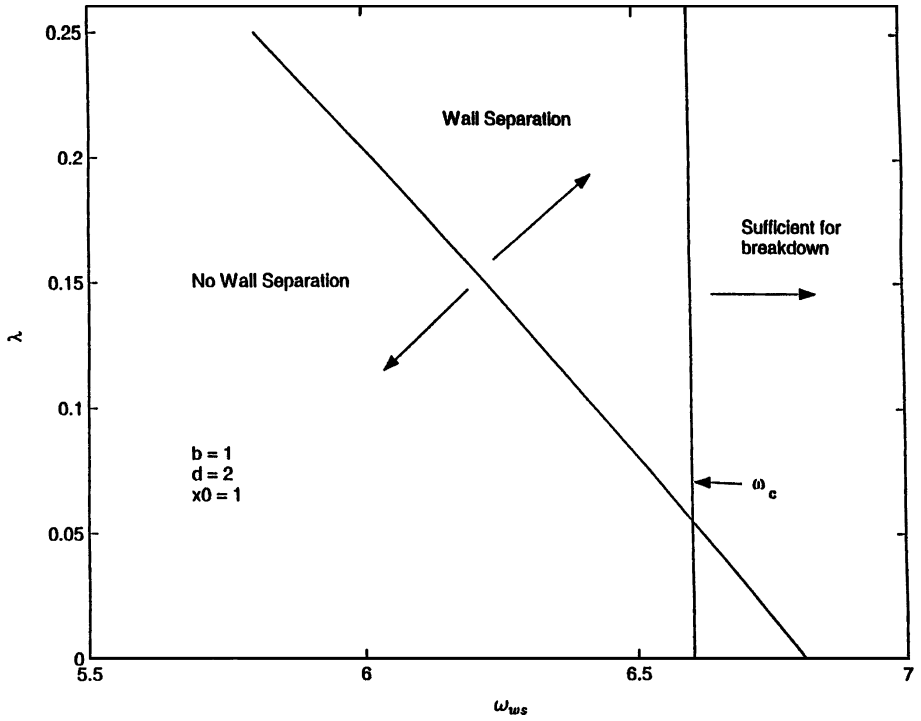

Fig. 5 Pipe contraction λ against the swirl level for wall separation ω_{ws} for an incoming Q vortex [Eq. (23)] with $b = 1.0$, $d = 2.0$ in a pipe with $x_0 = 1.0$.

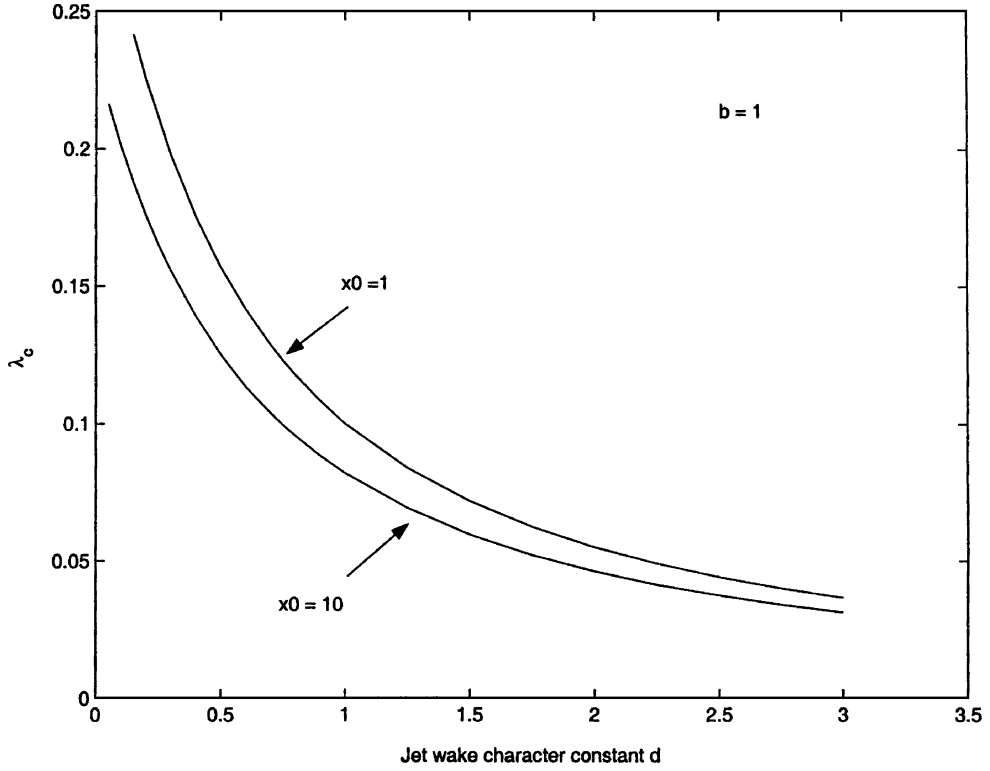

Fig. 6 The λ_c as a function of d for an incoming Q vortex [Eq. (23)] with $b = 1.0$ in pipes with $x_0 = 1.0$, 10.0.

at a fixed value of r_c. Again this shows that less pipe contraction is needed to find wall separation in vortex flows when the pipe length is greater.

V. Conclusions

The development of an inviscid, incompressible, axisymmetric, and near-critical swirling jet entering a slightly contracting pipe can be studied by asymptotic analysis. A nonlinear small-disturbance analysis is developed from the governing equations of motion and boundary conditions. It shows that a small but finite pipe contraction causes the flow to accelerate near the centerline and decelerate along the wall. For certain inlet vortex profiles and pipe contractions, the flow near the wall can stagnate. The analysis indicates for the first time that under certain pipe contractions a wall separation zone can appear at rotation levels below the critical swirl for vortex breakdown. The results demonstrate that pipe contraction helps to delay the onset of vortex breakdown near the pipe centerline to higher

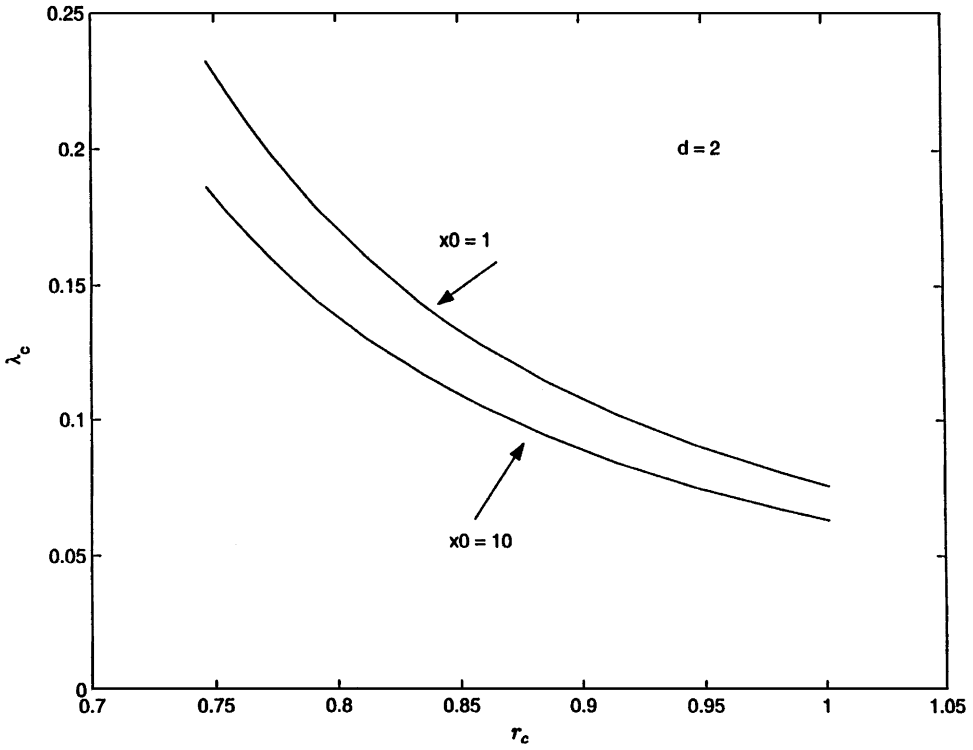

Fig. 7 The λ_c as a function of r_c for an incoming Q vortex [Eq. (23)] with $d = 2.0$ in pipes with $x_0 = 1.0, 10.0$.

swirl levels but can create wall separation zones that compete with the appearance of the breakdown zones. Increasing the vortex core radius, the speed of the axial jet, and the pipe length promotes the wall separation phenomenon at lower swirl levels for a fixed pipe contraction or at a smaller pipe contraction for a fixed swirl level. The analysis can be relevant for high-Reynolds-number laminar flows and as long as the boundary layers remain thin and attached to the pipe wall.

The computed results show that there can be certain physical conditions where wall separation zones can first appear as the incoming swirl level is increased. It is expected that in the range of swirl $\omega_{ws} < \omega < \omega_c$ these wall zones grow in size and move upstream with the increase of the swirl ratio. However, with further increase of the swirl ratio the flow can reach the critical swirl level for vortex breakdown ω_c. Based on the previous studies by Wang and Rusak[12] and Rusak et al. [13] on the vortex breakdown process, it is expected that at this swirl level the transition mechanism to breakdown can destabilize the flow state with a wall separation zone and dominate the flow dynamics. Then, the flow near the wall is accelerated, the wall separation zone will be convected out of the pipe, and a lower energy vortex breakdown state will be established in the pipe.

This dynamical scenario might help to explain the experimental phenomena found in the high-Reynolds-number swirling flows in a pipe studied by Mourtazin.[14] Large-amplitude standing waves adjacent to the pipe wall were found in these experiments at swirl levels below those where vortex breakdown was observed. These waves indicated the existence of a wall separation zone. As vortex breakdown suddenly appeared in the pipe with the increase of the incoming swirl level, these standing waves disappeared. The wall standing waves found in these experiments can be attributed to the significant flow contraction that characterizes the experimental apparatus of Mourtazin.[14] There, the flow is contracted from the settling chamber nozzle to the straight pipe downstream, and $\lambda \sim 0.25$. In addition, the envelope enclosing the wall standing waves reminds that describing the wall separation zones indicated by the present analysis when the pipe contraction is above the certain critical value λ_c and $\omega > \omega_{ws}$. It is clear however that inside the wall separation zone the present inviscid analysis is not relevant because the flow in this zone is dominated by viscous effects that form and determine the shape of the wall standing waves.

Finally, the present analysis together with Wang and Rusak's[12] study of swirling flows in a straight pipe show that the wall separation zones are not related to the occurrence of the vortex breakdown phenomenon and that the two phenomena are mostly independent one of the other. The wall zones can appear at certain conditions before breakdown appears. They disappear with the appearance of breakdown only because the breakdown state is a more stable, lower energy, dominant state that causes flow acceleration near the wall and the washout of the wall zones. Also, the wall zones do not necessarily precede vortex breakdown.

It is recommended to conduct further experimental, computational, and theoretical investigations to better clarify the interaction between these two complicated phenomena.

Acknowledgments

This research was carried out with the support of the National Science Foundation (NSF) under Grant CTS-9804745 and a supplemental award for C. C. Meder as part of the NSF Research Experiences for Undergraduates program.

References

[1]Hall, M. G., "Vortex Breakdown," *Annual Review of Fluid Mechanics*, Vol. 4, 1972, pp. 195–217.

[2]Leibovich, S., "Vortex Stability and Breakdown: Survey and Extension," *AIAA Journal*, Vol. 22, No. 9, 1984, pp. 1192–1206.

[3]Escudier, M., "Vortex Breakdown: Observations and Explanations," *Progress in Aerospace Sciences*, Vol. 25, 1988, pp. 189–229.

[4]Sarpkaya, T., "Vortex Breakdown and Turbulence," AIAA Paper 95-0433, Jan. 1995.

[5]Rusak, Z., "Review of Recent Studies on the Axisymmetric Vortex Breakdown Phenomenon," AIAA Paper 2000-2529, June 2000.

[6]Batchelor, G. K., *An Introduction to Fluid Dynamics*, Cambridge Univ. Press, Cambridge, England, U.K., 1967, pp. 543–555.

[7]Buntine, J. D., and Saffman, P. G., "Inviscid Swirling Flows and Vortex Breakdown," *Proceedings of the Royal Society of London*, Vol. 449, April 1995, pp. 139–153.

[8]Rusak, Z., Judd, K. P., and Wang, S.,"The Effect of Small Pipe Divergence on Near-Critical Swirling Flows," *Physics of Fluids,* Vol. 9, No. 8, 1997, pp. 2273–2285.

[9]Benjamin, T. B., "Theory of the Vortex Breakdown Phenomenon," *Journal of Fluid Mechanics*, Vol. 14, 1962, pp. 593–629.

[10]Leibovich, S., and Kribus, A., "Large Amplitude Wavetrains and Solitary Waves in Vortices," *Journal of Fluid Mechanics*, Vol. 216, 1990, pp. 459–504.
[11]Rusak, Z., and Judd, K. P., "The Stability of Non-Columnar Swirling Flows in Diverging Streamtubes," *Physics of Fluids*, Vol. 13, No. 10, 2001, pp. 2835–2844.
[12]Wang, S., and Rusak, Z., "The Dynamics of a Swirling Flow in a Pipe and Transition to Axisymmetric Vortex Breakdown," *Journal of Fluid Mechanics,* Vol. 340, 1997, pp. 177–223.
[13]Rusak, Z., Wang, S., and Whiting, C. H., "The Evolution of a Perturbed Vortex in a Pipe to Axisymmetric Vortex Breakdown," *Journal of Fluid Mechanics*, Vol. 366, 1998, pp. 211–237.
[14]Mourtazin, D., "Investigation of Vortex Breakdown of Swirling Flow in a Tube by the PIV Method," M.Sc. Thesis, Dept. of Aerospace Engineering, Technion—Israel Inst. of Technology, Haifa, Israel, June 1998.
[15]Beran, P. S., and Culick, F. E. C., "The Role of Non-Uniqueness in the Development of Vortex Breakdown in Tubes," *Journal of Fluid Mechanics*, Vol. 242, 1992, pp. 491–527.
[16]Beran, P. S., "The Time-Asymptotic Behavior of Vortex Breakdown in Tubes," *Computers and Fluids*, Vol. 23, No. 7, 1994, pp. 913–937.
[17]Lopez, J. M., "On the Bifurcation Structure of Axisymmetric Vortex Breakdown in a Constricted Pipe," *Physics of Fluids*, Vol. 6, No. 11, 1994, pp. 3683–3693.

H. Reed
Associate Editor